IPPI

Polyolefins Journal, Vol. 5, No. 2 (2018)
DOI: 10.22063/poj.2018.2047.1109

ORIGINAL PAPER

Effect of NH_3/methylaluminoxane/dodecylamine modified-nanoclay on morphology and properties of polyethylene/clay nanocomposites prepared by *in-situ* polymerization

Ali Alikhani, Shokoufeh Hakim*, Mehdi Nekoomanesh

Iran polymer and Petrochemical Institute, P.O. Box: 14975- 112, Tehran, Iran

Received: 23 October 2017, Accepted: 5 February 2018

ABSTRACT

This study presents methods for treating a kind of nanoclay and investigates the effects of methylaluminoxane (MAO) exposure time and or dodecylamine (DDA) reflux time on in-situ polymerization of ethylene in the presence of nanoclay and examines the morphology and properties of the prepared polyethylene/clay nanocomposites. The results revealed that by increasing MAO exposure time productivity decreased. Modification of nanoclay by NH_3/MAO led to formation of exfoliated structures. In treatment with NH_3/DDA, the change in reflux time resulted in different structures. SEM demonstrated that the morphology of the nanocomposites strongly depended on the modification method and treatment time. Dynamic mechanical analysis indicated that the elastic modulus of the nanocomposites increased by increasing MAO exposure time. The nanocomposites treated with different MAO exposure times showed similar thermal degradation behavior. The nanocomposite modified under the condition of 24 h DDA reflux time indicated the lowest thermal decomposition temperature due to poor dispersion of nanoclay in the synthesized nanocomposite. The nanocomposites modified by NH_3/MAO had higher degree of crystallinity compared to those modified by NH_3/DDA, which could be attributed to the difference in dispersion level of the modified clays. A relationship between the rheological properties, weight fraction and dispersion of modified nanoclay was observed. The findings showed that the modification condition had a significant influence on the morphology and properties of the synthesized nanocomposites. **Polyolefins J (2018) 5: 125-139**

Keywords: In-situ polymerization; polyethylene; nanoclay; methylaluminoxane.

INTRODUCTION

Polyethylene (PE) is one of the most widely used polymers due to its excellent chemical resistance, low dielectric constant, and low cost. However, it has some disadvantages such as low stiffness and tensile strength. Therefore, different modifiers are extensively used to improve different properties of PE [1–3].

Over the last decade, polymer nanocomposites have attracted great interest both in academic and industrial sectors. It is due to the fact that polymer nanocomposites possess considerably better performances compared to the conventional micro-composites[4]. Various types of nanofillers including graphene[5], polyhedral oligomeric silsesquioxane (POSS)[6,7], clay and carbon nanotubes [8, 9] have been incorporated into the polymer matrices to obtain materials with enhanced physical, mechanical, electrical and thermal

---

* Corresponding Author - E-mail: s.hakim@ippi.ac.ir

properties and also flame retardancy.

Investigation of properties of the PE/clay nanocomposites is the subject of numerous research studies in recent years [10–16].Two main methods have been employed for preparation of these nanocomposites: melt processing, and in-situ polymerization. In the former, the PE resin and nanofiller are mixed in the melt state, whereas in the latter, active sites of catalyst are supported on silicate layers, and therefore, macromolecular chains are formed between nanoclay galleries [17]. The major disadvantages of the melt processing are inadequate dispersion of nanoclay in the matrix, especially at high loadings, and the possibility of thermal degradation of the matrix [18]. In contrary, in-situ approach can provide good filler dispersion due to an increase in the gallery space between the clay layers during polymerization process. Furthermore, it allows researchers to design polymers with desirable microstructures using different catalysts [15, 19]. Therefore, in-situ polymerization of the ethylene using Ziegler–Natta, and metallocene catalysts supported on the layered silicates has been extensively studied [20-25]. However, in-situ polymerization has caused some problems such as excessive consumption of cocatalyst, and low activity. In fact, water content of the layered silicates is an important issue in the in-situ polymerization, because it acts as a catalyst poison. On the other hand, homogeneous dispersion of the active sites on the nanoclay surface, and their extraction from support surface are important issues that need to be addressed in the in-situ polymerization [19,26, 27]. Therefore, modification of nanofiller and catalyst supporting method are key parameters for achieving nanocomposites with high performance properties.

Modification of nanoclay using organic cations is one of the most common routes to improve fixation of the catalyst between the silicate layers. There are reports on the nanoclays modified with octadecylamine (ODA)[28], alkylammonium [29], glycinate hydrochloride [30], undec-10-enylammonium chloride (as a polymerizable organic modifier) [31], and organosilane[32]. It was reported that the catalytic activity of the metallocenes supported on ODA-treated nanoclay during in-situ polymerization of ethylene was comparable to that of those without nanofiller [28]. Also, Ren et al. [33] synthesized a multi-functional ammonium modifier with carbonyl and vinyl groups to treat montmorillonite (MMT). Polymerization of ethylene in the presence of the modified MMT resulted in exfoliated structures even at very high nanoclay content, which was attributed to the high level of metallocene anchoring within the interlayer of MMT due to the presence of carbonyl groups.

Some researchers have used aluminoxanes to modify different nanoclays [29,34-37]. Leone et al. [34] investigated the influence of the nanoclay pretreated by methylaluminoxane (MAO) on the properties of PE nanocomposites. They found out that the catalytic activity for the nanocomposite was higher than that for neat polymer. Moreover, the catalytic activity was enhanced by increase in the contact time between MAO and Cloisite 15A. As mentioned earlier, this type of modification requires high volumes of MAO to obtain good polymerization activities [19]. In another treatment approach, the partial hydrolysis of alkyl aluminums with the water molecules of the nanoclay surface provided high activities[38-41]. Maneshi et al. [26] reported a catalyst supporting method for different nanoclays that did not require incorporation of MAO. The authors found that only the catalyst supported on Cloisite 93A showed a high polymerization activity because, contrary to other nanoclays modified with quaternary ammonium, this nanoclay with tertiary ammonium salts in its gallery possesses water molecules which can form MAO by reaction with alkyl aluminum.

In our previous work [15], a new method was presented for treatment of the clay nanoplatelets using ammonia gas and dodecylamine (DDA). The activity of the catalyst supported on the treated nanoclay was much higher than that supported on Cloisite 15A, and an exfoliated structure was obtained for PE nanocomposites. Furthermore, a recent work of our lab [42] reveald that NH_3 together with MAO and DDA (as modifiers of the nanoclay) are effective factors on the activity of metallocene in polymerization of ethylene. In continuation of our research on this area, now, we report different procedures for modification of Na-MMT and investigate effects of the modification parameters (MAO exposure time and DDA reflux time) on the morphology and properties of the prepared PE nanocomposites.

EXPERIMENTAL

Materials

The zirconocene catalyst "bis (cyclopentadienyl) zirconiumdichloride" (Cp_2ZrCl_2) and methylaluminoxane (MAO, 10 wt.% in toluene) were supplied by Aldrich (Germany). Toluene was the product of Bandare-e-Imam Petrochemical Company (Iran). Dodecylamine (DDA) ($CH_3(CH_2)_{11}NH_2$) was obtained from Merck (Germany). Na-MMT with cation exchange capacity (CEC) of 92 meq/100 g, interlayer spacing of 1.17 nm and moisture content of < 2.00 wt% was purchased from Southern Clay Products (USA). Ammonia gas was purchased from Roham Gas Company (Iran).Nitrogen and ethylene (industrial grades) were obtained from Bandar-e-Imam Petrochemical Company. Ammonia was dried by passing through columns of active calcium carbonate, potash and soda. Also, nitrogen and ethylene were purified by passing through a 4 Å molecular sieve column.

Preparation of nanocomposites

Modification of nanoclay

All experiments were performed under nitrogen atmosphere in a glove box under argon atmosphere. At first, 0.5 g of Na-MMT was dispersed in 200 cc toluene by stirring. The suspension was then exposed to ammonia gas for 30 min at room temperature. After that, it was heated at 110°C for 1 h and also washed with fresh toluene three times to remove unreacted ammonia. The wet filtrated nanoclay was dried in an oven at 100°C for 30 min. In the case of the modification with dodecylamine, 0.5 g of DDA was dispersed in 10 cc toluene. After that, 0.5 g of NH_3-modified clay was added to the DDA solution and the mixture was stirred under reflux at boiling point of toluene (78°C) for 24, 48, and 72 h, respectively. The precipitated solid was filtered and washed with toluene three times to remove unreacted DDA. In the modification with methylaluminoxane, 0.5 g of NH_3-modified clay and 1 cc of MAO were added to 10 cc of toluene. The stirring process was carried out for 2, 4, and 6 h, respectively at room temperature. Then, the solution was rested in stationary condition to permit precipitation of clay. The unreacted MAO was washed with fresh toluene three times and the excess amount of toluene was removed.

Supporting process

In this step, 0.01 g of metallocene catalyst (Cp_2ZrCl_2) was dissolved in 10 cc of toluene. Then, the solution was added to 0.5 g modified clay slurried in toluene and stirred for 2 h at room temperature. Finally, the mixture was washed with toluene three times to remove unreacted metallocene catalyst. The catalyst supported on the modified clay was named pre-MMT-Zr.

Polymerization

The polymerization of ethylene was carried out using pre-MMT-Zr and additional 5 cc of MAO in a 1 L Buchi stainless steel reactor equipped with magnetic drive stirrer (model bmd 300) and an anchor agitator. Before polymerization, the reactor was heated up to 90°C and purged with argon for 1 h. Then, the reactor was cooled down to 65°C (polymerization temperature) and purged again with argon for 1 h. After that, 400 cc of toluene was charged into the reactor. 5 cc of MAO was added and stirred for 5 min. In the next step, the supported catalyst slurry was introduced to the reactor and ethylene gas was regulated at 4 bar. After 1 h, the polymerization was terminated by reducing monomer pressure. The polymerized nanocomposite was washed with methanol and dried in a vacuum oven at 80°C for 24 h. The clay modification and ethylene polymerization conditions are shown in Table 1. It is necessary to note that the codes of the samples containing nanoclay modified with NH_3, NH_3/DDA and NH_3/MAO are MD0, M2-M6 and D24-D72, respectively.

The nanoclay weight percentage (NC_{wt}) in the in-situ polymerized samples was calculated using the following equation:

$$NC_{wt} = \frac{0.5}{P} \times 100$$

where NC_{wt} is the weight percentage of nanoclay in the produced polymer, and P is the amount of the produced polymer. Also, 0.5 refers to the weight of the nanoclay added to the reactor, which was 0.5 g for all samples.

Characterization

Molecular weight measurement

To measure the viscosity average molecular weight

Table 1. Modification and polymerization conditions.

Samples Codes	MAO amount used in pretreatment stage (cc)	MAO exposure time (h)	DDA amount used in pretreatment stage (g)	DDA reflux time (h)	Produced polymer (g)	Yield (g/gclay t)	Nanoclay wt.% in polymer
MD0	-	-	-	-	20	40	2.5
M2	1	2	-	-	117	234	0.42
M4	1	4	-	-	73	146	0.68
M6	1	6	-	-	46	92	1.08
D24	-	-	0.5	24	12	24	4.1
D48	-	-	0.5	48	52	104	0.96
D72	-	-	0.5	72	30	60	1.66

Clay=0.5 g, MAO in polymerization=5cc, Catalyst=0.01 g.
All samples exposed to NH_3 for 30 min.

(M_v), the samples were dissolved in decaline (0.02 $g.dL^{-1}$) at 165ºC and then filtered through a 0.2 mm paper filter to remove the clay in order to avoid the errors due to the presence of clay particles. Then, the solution was quickly transferred to an Ubbelohde viscometer at 135ºC. M_v was calculated according to the Mark-Kuhn-Houwink equation ($[\eta] = k (M_v)^{\alpha}$ with $k = 6.2\times10^{-4}$ and $\alpha = 0.7$).

Scanning electron microscopy (SEM)

To investigate morphology of the nanocomposites, the samples were sputter coated with gold and examined using a Vega Tescan model scanning electron microscope.

X-ray diffraction (XRD)

XRD measurements were carried out using a Siemens D 500 diffractometer (Germany) equipped by Cu Kα radiation at the voltage of 40 kV and current of 40 mA. The diffractograms were scanned in the 2θ range of 1.5° to 10°, at the rate of 1°/min, and at ambient temperature. The measurements were recorded with a step size of 0.02°.

Thermal gravimetric analysis (TGA)

TGA measurements were performed by a TGA-PL 1500 instrument. The samples were heated up to 600°C under the heating rate of 10°C min^{-1}.

Differential scanning calorimetry (DSC)

The melting behavior of the nanocomposites was investigated by a NETZSCH DSC 200 F3 instrument (Germany).The samples were first heated (with a rate of 10 $K.min^{-1}$) from 25°C to 180°C and then were cooled (with a rate of 10 $K.min^{-1}$) to 25°C. Then they were again heated (with a rate of 10 $K.min^{-1}$) to 180°C.

Dynamic mechanical analysis (DMA)

Dynamic mechanical properties were studied using a Tritec 2000 DM instrument (England) from –150 to 150°C at a heating rate of 5°C.min^{-1} and frequency of 1 Hz.

RESULTS AND DISCUSSION

Polymerization using catalyst supported on treated nanoclay

The successful polymerization of ethylene in the presence of nanoclay is best achieved when the metallocene catalysts are supported efficiently on the platelets of layered silicates, which, in turn, leads to higher activity and yield [15]. According to Table 1, the highest content of the produced PE or yield is observed for M2 sample, which means that MAO exposure time of 2h had the best efficiency. In fact, a significant increase in the yield of this sample (approximately 6 times) can be observed compared to that of the sample containing nanoclay modified with NH_3. Moreover, as the MAO exposure time increases, the amount of synthesized PE decreases. Therefore, it appears that 2 h is sufficient time for modification of Na-MMT with MAO. On the basis of the amount of the produced polymer, the efficiency of the modification processes could be ordered as follows:

$$M2 > M4 > D48 > M6 > D72 > MD0 > D24$$

Treatment of the Na-MMT with NH_3 introduces ammonia molecules into the nanoclay galleries. In fact,

NH_3 can create the hydrogen bonding with the water molecules and as a result, an NH_3-water azeotrope is formed which is then extracted from clay galleries by heating at higher temperature. On the other hand, the presence of NH_3 around water molecules generates a shielding effect that prevents the metallocene from being poisoned [15,42]. The FTIR spectra in our recent work [42] showed that the treatment with NH_3 decreased the intensity of peaks related to the hydrogen-bonded water molecules and interlayer water deformation in the nanoclay.

MAO is a mixture of linear and cyclic oligomers of different lengths [43]. It enters into the reaction with silanol functional groups of the Na-MMT surface and forms oxygen-aluminum bonds. By the incorporation of metallocene, the reaction between the catalyst molecules and MAO deposited on the clay surface leads to formation of alkyl zirconocene cations which are active sites for ethylene polymerization. Therefore, treatment of the nanoclay with MAO for 2 h provides an appropriate medium to create active sites on the surface of Na-MMT. Moreover, in the presence of MAO, the concentration of free hydroxyl groups is very low and as a result, deactivation of the active sites decreases significantly [42]. So, one of the main reasons for the lower activity of the catalysts supported on the nanoclays treated with NH_3 and NH_3/DDA (MD0 and D24-D72 samples) compared to those treated with NH_3/MAO (M2-M6 samples) is the fact that in the former samples, the degree of metallocene deactivation with hydroxyl groups is higher.

As observed, the higher MAO exposure times led to producing a smaller amount of polymer. The explanation for this observation is as follows: When the MAO exposure time increases up to a certain value, the activity increases because MAO can stabilize the active sites of the catalyst. In contrast, at higher exposure times, the content of the co-catalyst on the nanoclay surface increases. In this case, there is a possibility of deactivation of the active sites, as shown in Figure 1 [44]. On the other hand, the presence of higher content of MAO in the nanoclay galleries hinders the introduction of catalyst into the interlayer space of Na-MMT, causing lower supporting efficiency and yield of the polymerization [28].So, M4 and M6 samples showed lower productivity than the M2.

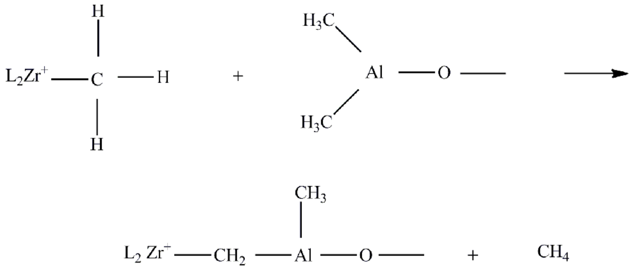

Figure 1. Deactivation of the active sites by excess MAO [44].

The results of modification with NH_3/DDA revealed that by increasing the reflux time from 24 to 48 h, the amount of produced PE increased, whereas further increase resulted in a reverse effect. The treatment with DDA having long hydrocarbon chain increased the interlayer space of Na-MMT and as a result, the supporting of the catalyst on the nanoclay layers took place more easily. Similar to the modification with NH_3, the treatment with NH_3/DDA reduced the water content in the nanoclay. DDA molecules also have the ability to react with the functional groups on the nanoclay surface, which was verified by the appearance of the band at 3000 cm^{-1} belonging to the N–C and N–H groups [42]. On the other hand, the insertion of ethylene monomer into the interlayer space and reaction with the active centers located in the internal points of the modified nanoclay increased. Also, DDA molecules play the role of spacer groups of the catalyst, and thus can decrease the deactivating bimolecular reactions [28]. Furthermore, the presence of the DDA modifier improved the compatibility between the polymer chains and nanoclay, which is crucial for the preparation of nanocomposites. The decline in the yield of D72 sample could be attributed to the role of amine functional groups of DDA in deactivating active sites [28]. In other words, the negative effect of DDA on the activity could be stronger than its positive effect after an optimum level of reflux time.

The molecular weights of the prepared samples are presented in Table 2. As seen, M2 has the highest M_v, and also the molecular weight is decreased by increasing the MAO exposure time. This can be due to the reasons mentioned above. In fact, by modifying the nanofiller, the sheets of layered silicates are separated from each other and thereby, the chain growth reaction is facilitated. Thus, by considering the effects of the exposure times of MAO and reflux times of DDA (as

Table 2. Crystallinity, melting temperature and viscosity average molecular weight (M_v) of PE samples.

code of sample	T_m[1] (°C)	ΔH_m[2] (J/g)	X_c[3] (%)	$M_v \times 10^{-3}$ (g/gmol)
M2	129.8	212.3	72.4	83.4
M4	130	213.7	72.9	48.9
M6	131.4	208.2	71	26.2
D24	134.8	182.2	62.1	61.9
D48	134.9	187.7	64	66.1
D72	132.9	192.7	65.7	50.9

(1) Melting temperature
(2) Melting enthalpy
(3) Crystallinity

described before), it can be observed that there is a direct relationship between the modification efficiency and molecular weights of the samples.

Morphology

The SEM micrographs of the nanocomposites containing nanoclay modified with NH_3 are shown in Figure 2. Lower activity and less particle growth resulted in increasing of surface area and tending to agglomeration. The nanocomposites show a special morphology with porous surfaces. It is probably due to replicating of the nanoclay-supported catalyst. The modification of nanoclay with NH_3/MAO leads to creation of different morphologies (Figure 3) completely different from the morphology of pure PE. Fragmentation has not seen as much as in pure PE. It can be because of the enhancement in the heat and mass transfer in the supported catalyst due to the porosity of nanoclay. For these nanocomposites, less agglomeration was observed compared to the nanocomposites modified with NH_3. By increasing the MAO exposure time, significant changes took place in the morphology. For M2, the growing of the particles was successful and the induced tensions led to fragmentation of particles. This observation is in total agreement with high activity of catalyst (117 g) in this condition. The morphology of the M4 and M6 nanocomposites reveals less fragmentation compared to that observed for the M2.

In the case of the modification with NH_3/DDA, the morphologies are completely different from the other cases (Figure 4). In fact, different morphologies are observed for different DDA reflux times. This may be attributed to the presence of amine functionality and formation of inter-molecular hydrogen bonding. Furthermore, long carbon chains in the DDA structure can lead to the formation of this morphology. The comparison of the morphologies related to different DDA reflux times indicates slightly fragmentation for D48 nanocomposite. This is consistent with that observed for the produced polymer (52 g). Degree of fragmentation depends on the catalyst activity directly and on the shielding of hydroxyl groups indirectly, which prevents poisoning of catalyst. In addition, it seems that the chemical nature of modifying agent is vital factor in the formation of final morphology, i.e. MAO

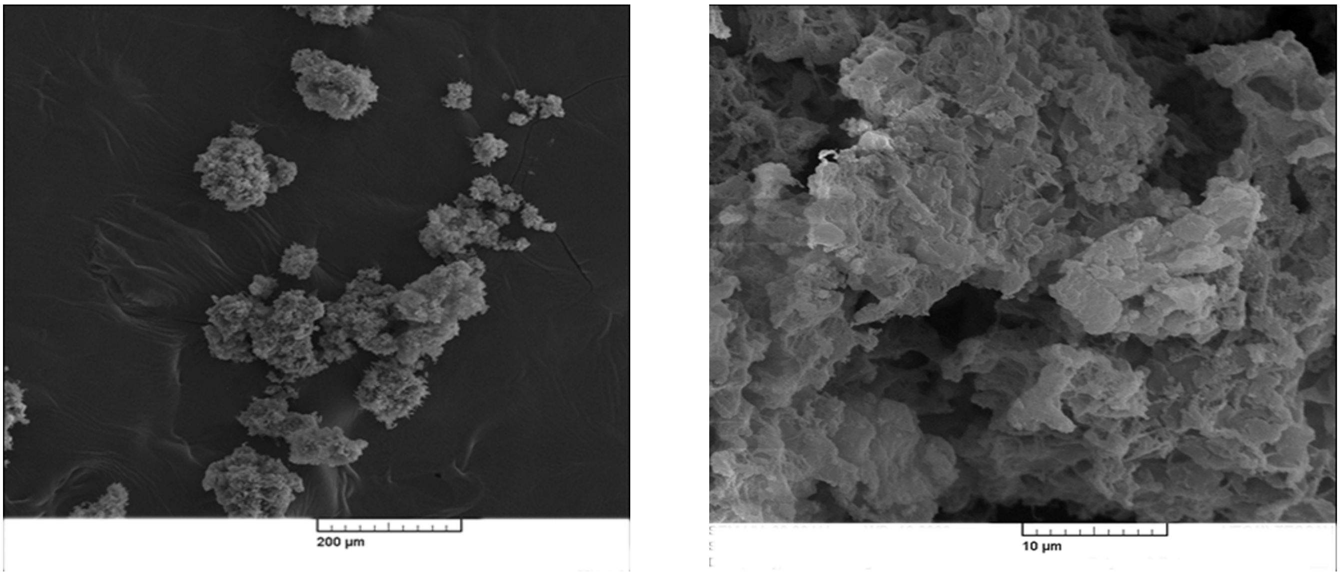

(a)

(b)

Figure 2. SEM micrographs of nanocomposites containing nanoclay modified with NH_3 (MD0) at (a) low and (b) high magnifications.

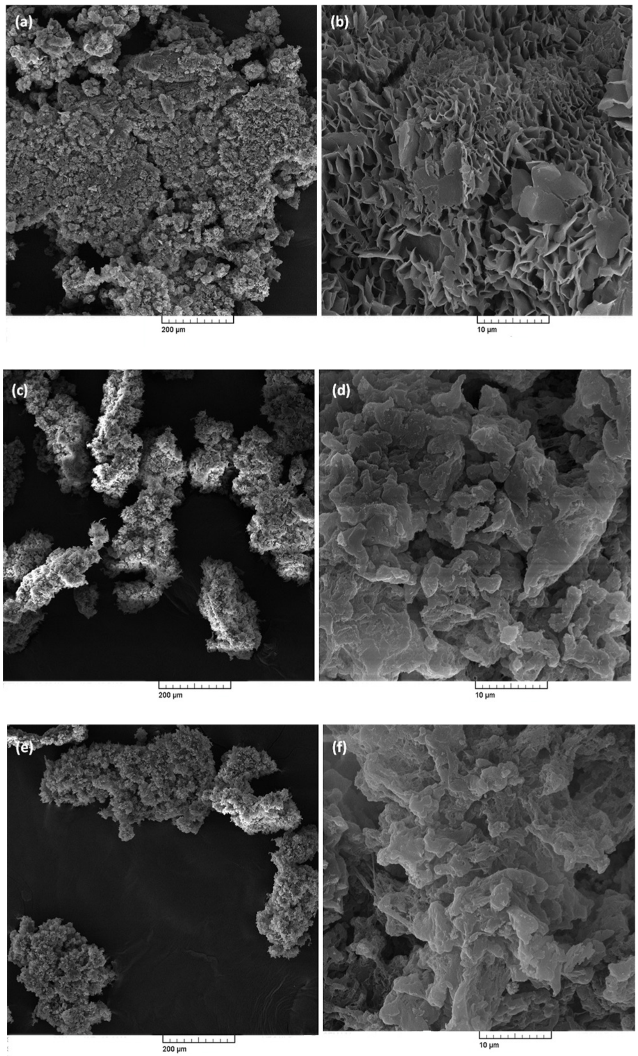

Figure 3. SEM micrographs of (a,b) M2, (c,d) M4, and (e,f) M6.

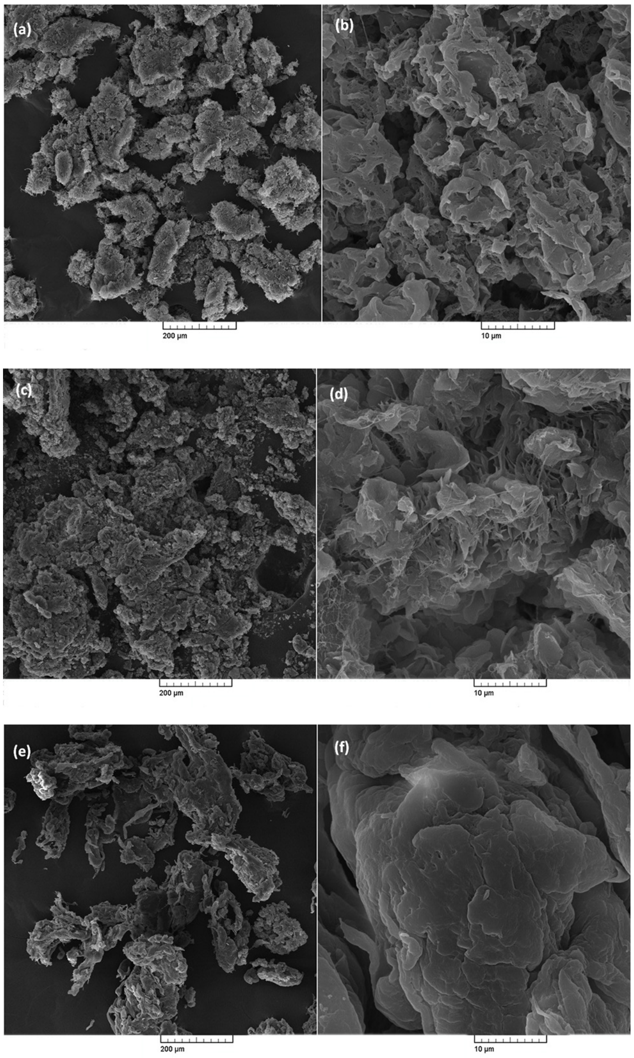

Figure 4. SEM micrographs of (a,b) D24, (c,d) D48, and (e,f) D72.

treatment tends to change morphology from a special shape in lower activities to a fully fragmented morphology in high activities, and a flag-like morphology was observed in the case of DDA and NH_3 treatments. The comparison of the M2 and D48 nanocomposites revealed that the degree of fragmentation was higher in the former. This could be related to the higher amount of the polymer produced in the case of modification with MAO.

X-ray diffraction (XRD)

To assess the dispersion level of the nanoclay particles in the PE matrix, the prepared nanocomposites were investigated by XRD. Figure 5 shows the X-ray patterns of the neat Na-MMT and nanocomposites containing nanoclays pretreated by the different modification methods. As seen, the neat Na-MMT shows a characteristic peak at $2\theta=7.4°$. By using Bragg's law (equation 1), d-spacing of 11.7 Å could be calculated for this nanoclay:

$$d = \frac{\lambda}{2\sin(\theta)} \qquad (1)$$

Where d is the distance between layers, and λ is the wavelength of X-ray beam. For the MD0 sample (modified by NH_3), the characteristic peak of the nanoclay is shifted to $2\theta=3.34°$ corresponding to an interlayer spacing of 26.5 Å. This observation indicates that the distance between the nanoclay layers considerably is increased and intercalated structures are obtained. It is attributed to effective treatment of nanoclay and polymerization of monomer in the interlayer space. The pressure exerted by the PE chains causes separating of

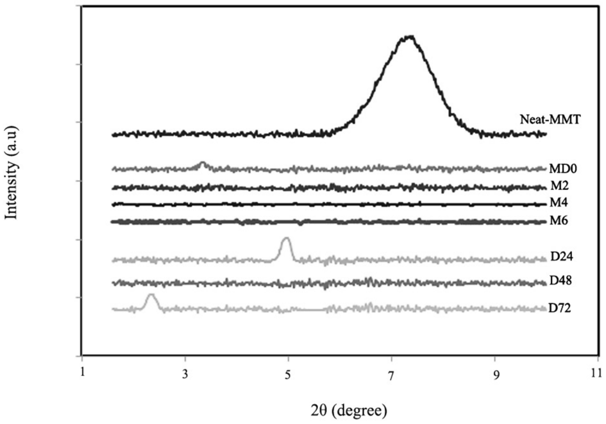

Figure 5. X-ray patterns of neat Na-MMT and nanocomposites containing nanoclays.

the layers, and therefore, to increasing of d-spacing.

In-situ polymerizations on the surface of nanoclay treated with NH_3/MAO caused to obtain a completely disordered structure which was verified by the XRD spectra. Therefore, it could be concluded that the exfoliation of the platelets was occurred in the M2, M4, and M6 nanocomposites. Since the activity of the catalyst obtained by this modification method was much higher than the activity of those catalysts obtained by the other methods, the high amount of produced PE chains increased the interlayer space and generated a significant disorder in the structure of the nanoclay. In fact, this type of treatment provides the exfoliation of the nanoclay through catalyst activation and appropriate growth of the PE chains. Furthermore, the percentage of nanoclay in these samples is very low (Table 1) and as a result, the possibility of agglomeration of the platelets is small.

Among the nanoclays modified with NH_3/DDA, D48 sample also presented a completely disordered pattern, suggesting the existence of exfoliated structure. The spectrum of the D24 nanocomposite exhibited a peak at 2θ=4.96°. The reason is the low content of the polymer produced within the interlayer space, which, in turn, applies a small force to separate layers. In the D72 nanocomposite, the characteristic peak corresponding to the modified MMT appeared at 2θ=2.38° (d-spacing of 37.5 Å). Therefore, it can be said that the degree of intercalation in this nanocomposite is higher than that in the MD0 nanocomposite.

It is deduced that the XRD patterns are in good agreement with the results obtained by the morphology testes. In other words, the optimum modification approach could provide catalyst with high activity and productivity, resulting in larger interlayer space and good dispersion of layered silicates in the PE matrix.

Dynamic mechanical analysis (DMA)

The temperature-dependency of storage modulus for various PE/nanoclay nanocomposites is illustrated in Figure 6. According to Figure6a, the elastic modulus of the nanocomposites increases by increasing the MAO exposure time. Since all of the M2, M4, and M6 samples showed exfoliated structures, this behavior could be attributed to the nanoclay content in the final nanocomposite. As it is clear in Table 1, the content of produced polymer decreases with increasing the MAO exposure time and as a result, the percentage of nanoclay in the nanocomposite increases. Therefore, the samples with a higher content of modified nanoclay show higher elastic modulus, because the nanoclay platelets hinder the movement of the chains. The interesting point is that the viscoelastic behaviors of the nanocomposites containing Na-MMT modified by NH_3/MAO are the same. It is originated from the exfoliated structure of the layered silicates in these nanocomposites as evidenced by the XRD patterns too.

Figure 6b reveals that the variation of elastic modulus for the D24 nanocomposite (DDA reflux time of 24 h) completely differs from those for the D48 and D72 nanocomposites. Additionally, this sample had a much higher elastic modulus compared to other samples. This observation can be explained by the difference in the degree of dispersion and content of the nanoclay in these samples. In fact, the nanofiller particles were in the form of a partially intercalated structure for the D24, whereas the D48 and D72 nanocomposites showed a much better dispersion of the nanoclay within the matrix. Moreover, the high percentage of nanoclay in the D24 (4.1%) due to low catalyst activity was the origin of high modulus in this nanocomposite.

Thermal gravimetric analysis (TGA)

Figure 7 depicts the TGA thermograms of different synthesized samples. The residue obtained from the thermal degradation of the PE/nanoclay nanocomposites consisted of carbon, nanoclay, oxidized metals,

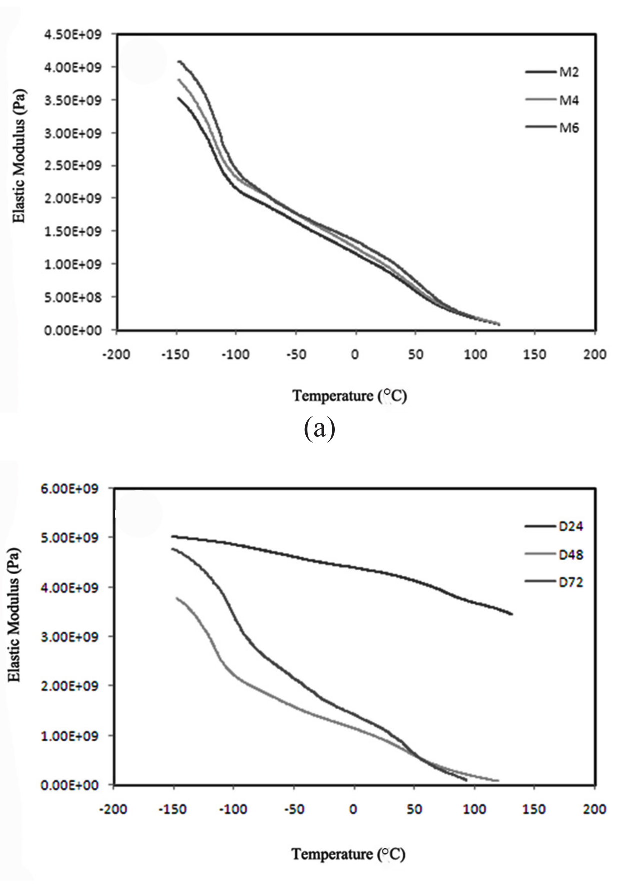

(a)

(b)

Figure 6. Temperature dependence of storage modulus for (a)M2-M6 and (b) D24-D48.

and Al(OH)3 (obtained from the decomposition of MAO)[45]. As seen in Figure 7a, there are little differences between the TGA profiles of the nanocomposites reinforced with nanoclay modified by NH_3/MAO. Nevertheless, the M6 nanocomposite shows a lower thermal stability in the temperature range of 100-400°C. In this temperature range, the weight loss is related to the degradation of the modifier of the nanoclay. Since M6 contains higher nanoclay content, it is expectable that higher gaseous products are emitted during the thermal decomposition. On the other hand, M4 exhibits higher thermal stability (higher T_{onset} and T_{max}) in the range of 400-500°C, which corresponds to the degradation of the PE chains. It appears that, in spite of the lower concentration of the treated nanoclay in this nanocomposite (0.68%) compared to M6 (1.08%), the thermal stability of the matrix was improved more efficiently by this nanocomposite due to its higher exfoliation degree. The M6 nanocomposite shows higher ash content than other samples due to higher percentage of nanoclay in this sample.

From the TGA thermograms (Figure 7b), it is obvious that the D24 nanocomposite possesses the lowest decomposition temperature and the highest ash content. This could be related to the poor dispersion of the nanoclay in the PE matrix. Therefore, the nanoclay particles couldnot act as barriers during the TGA test. Also, the presence of stacked layered silicates can cause accumulation of heat in the matrix leading to accelerated degradation [46].Therefore, the TGA results can be used to conclude that there are more agglomerates than individual layers in this nanocomposite. It is well known that nanoclay has two opposite effects on thermal degradation of the polymer nanocomposites. The first one is the barrier effect of platelets that enhances thermal stability of the matrix, whereas the second one correlates with the catalytic or promoting effect that intensifies degradation. At low nanoclay content, the barrier effect is stronger owing to appropriate dispersion of the layers. Catalytic effect is

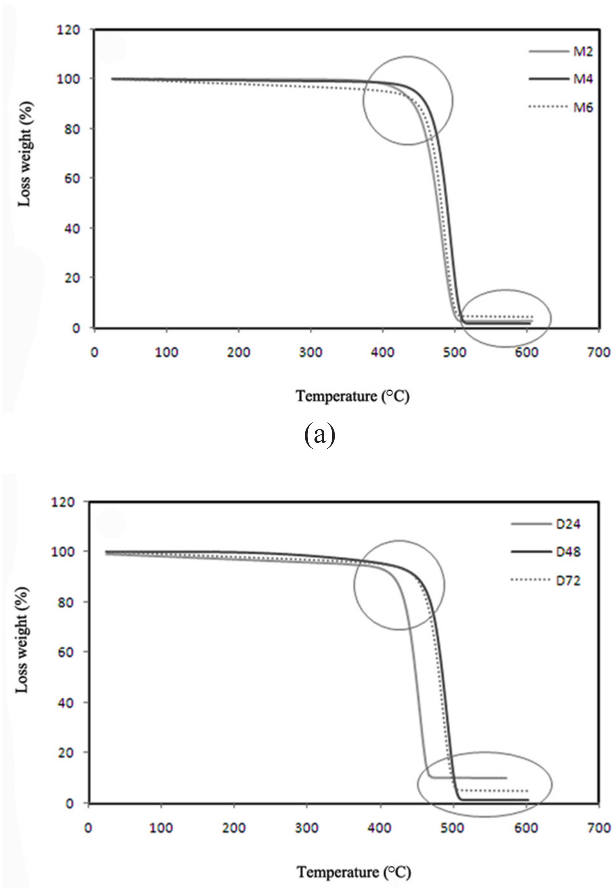

(a)

(b)

Figure 7. TGA thermograms of (a)M2-M6 and (b) D24-D48.

dominant at high contents [47]. Therefore, it appeared that the catalytic effect decreased the thermal stability of this nanocomposite because of high concentration of nanoclay (4.1%) in the nanocomposite.

The D48 and D72 nanocomposites had higher thermal stability compared to D24 sample. As explained earlier, they showed exfoliated and highly intercalated structures, respectively. In fact, the barrier effect of the modified Na-MMT prevents the decomposition of PE matrix, leading to increase in the T_{onset} and T_{max} for D48 and D72 samples. In other words, the polymer chains close to the nanoclay sheets degrade slowly. Therefore, the more efficient the barrier effect, the better is the dispersion of the nanoclay.

Differential scanning calorimetry (DSC)

The melting behavior of the nanocomposites is shown in Figure 8. Also, the characteristic data including melting temperature (T_m), melting enthalpy (ΔH_m), and degree of crystallinity (X_c) are presented in Table 2. The degree of crystallinity of PE was calculated based on the following equation:

$$X_c = \frac{\Delta H_m}{\Delta H_m^{\circ}} \times 100\% \qquad (2)$$

Where ΔH_m is the measured melting enthalpy of the sample and ΔH_m^0 is the melting enthalpy of 100% crystalline PE (293 J/g [48]). It can be seen that the melting temperature and degree of crystallinity of the M2 and M4 nanocomposites are very close to each other. By increasing the MAO exposure time to 6 h (M6), the melting temperature increases and the degree of crystallinity decreases. Moreover, the degree of crystallinity of D24 nanocomposite is lower than those of the other nanocomposites filled with nanoclay treated by NH_3/DDA. Similar to the thermal stability, layered silicates influence the crystallization behavior of nanocomposite through different mechanisms: (1) nanoclay can act as nucleating agent and help to create perfect crystallites and increase their numbers. (2) The interaction between the nanoclay and polymer chains hinders movement of the macromolecules and decreases their crystallization [16, 49]. Nanoclay loading and dispersion level are the factors determining the competition between these mechanisms. It has been reported that high nanoclay loading is in favor of the second mechanism [50]. So, higher percentage of the nanoclay in D24 sample causes less growing of the crystallites. However, this sample showed the highest melting temperature. It is due to the formation of much thicker lamellar structures. Similar observation has been reported by Lee et al. [51] for the PE/ clay nanocomposites prepared by melt processing.

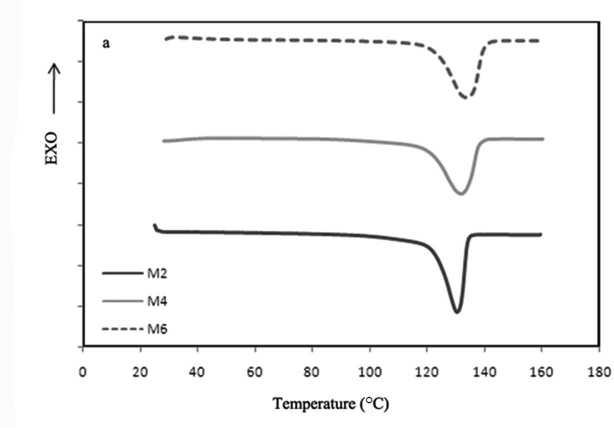

(a)

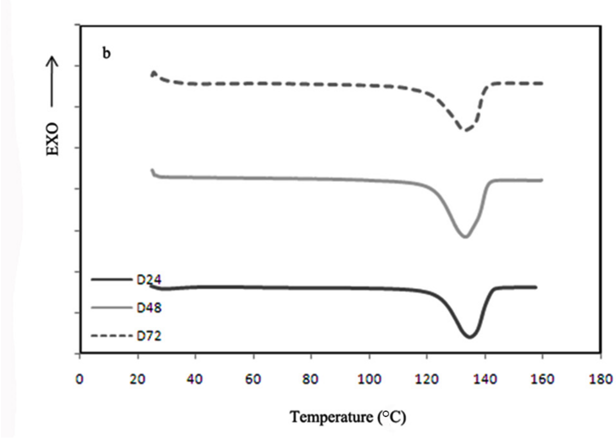

(b)

Figure 8. Melting behavior of (a)M2-M6 and (b) D24-D48.

The interesting finding is that the degree of crystallinity of the nanocomposites containing nanoclay modified by NH_3/MAO is higher than those of the samples treated with NH_3/DDA. It could be ascribed to the differences between the dispersion levels of the nanoclay in these nanocomposites. M2-M6 samples which have low nanoclay contents showed exfoliated structures, whereas D24-D72 nanocomposites which have high nanoclay contents were less exfoliated/or intercalated structures. Therefore, it is reasonable that the former category has higher degree of crystallinity. For the latter group, the effects of the aforementioned mechanisms are counteracted or even the second mechanism dominates.

Rheological properties

Investigation of the rheological properties can provide useful information on processability of the prepared nanocomposites. Figure 9a shows the complex viscosity of the samples as a function of frequency. As observed, the order of the samples according to their complex viscosity values at low frequencies are as follows:

M6>D48>D72>M2>D24>M4

The two factors that should be considered to interpret the results are dispersion and content of the nanoclay. According to the results deduced from the XRD patterns, all of the nanocomposites containing nanoclay modified with NH_3/MAO (M2-M6) showed exfoliated structures and M6 sample possessed the highest nanoclay content (1.08 %). Therefore, it had the highest complex viscosity at low frequencies. The curve slope at low frequencies for M6 is higher than those for the other samples. Furthermore, this nanocomposite showed a strong shear-thinning behavior. In fact, the presence of the nanoclay particles in the polymer matrix increased the viscosity at low frequencies. On the other hand, high shear rates force the layered silicates to align parallel to the flow direction and as a result, the viscosity is reduced [46, 52]. Therefore, M6 with the highest clay content showed the highest viscosity among the samples. Also, at high shear rates, the alignment of the nanoclay particles is more widespread for M6 nanocomposite than the other samples, leading to a significant loss in viscosity.

Also, the nanoclay particles were exfoliated and intercalated in D48 and D72 nanocomposites, respectively, whereas the nanoclay content was higher in the latter one. However, the D48 had a higher complex viscosity than that of the D72. Although, M2 and M4 samples had a good dispersion of the nanofiller in the PE matrix, but a very low concentration of the nanoclay led to low values of complex viscosity. Moreover, in spite of the high nanoclay content in the D24, a relatively low complex viscosity was obtained for this nanocomposite due to weak dispersion of the nanoclay. The results suggest that a good degree of dispersion and nanoclay content ≥~1 % can result in high melt viscosity.

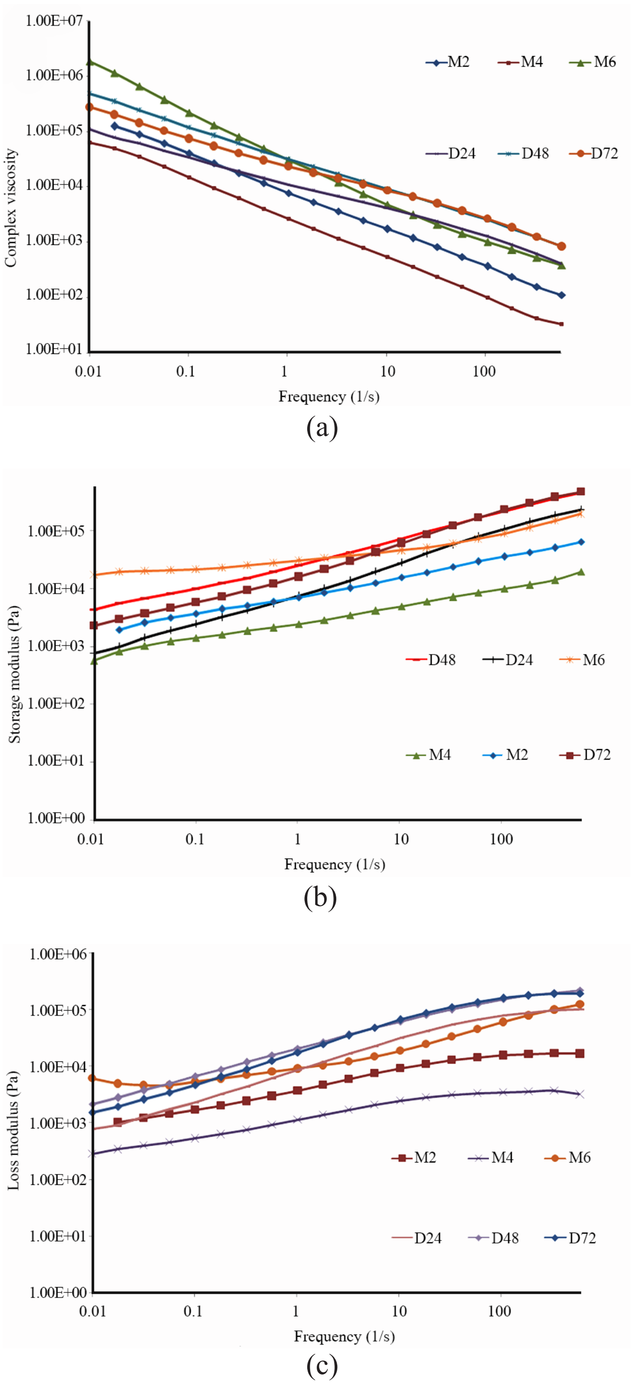

(a)

(b)

(c)

Figure 9. Complex viscosity, storage modulus and loss modulus of nanocomposites.

Figure 9 (b, c) shows storage and loss moduli of the nanocomposites. The trends observed for the storage and loss moduli are the same as those observed for the complex viscosity. M6 nanocomposite shows a solid-like behavior at low frequencies with the highest storage modulus and the lowest frequency-dependence. It can be ascribed to the formation of high density network of nanoclay platelets in the matrix that increases the elasticity of nanocomposite [35].

CONCLUSION

In this work, PE/clay nanocomposites were prepared by in situ polymerization and the influence of nanoclay modification method on the final properties of resultant nanocomposites was comprehensively studied. Increase in the MAO exposure time caused a loss in the yield of the PE and its molecular weight. Also, by increasing the DDA reflux time, the aforementioned parameters were first increased and then decreased. Due to the differences between the activity of the catalysts, and the interaction between the polymer and modified nanoclay, different XRD patterns were observed. In fact, treatment of the nanoclay with NH_3/MAO provided exfoliated structures through appropriate catalyst activation. An exfoliated structure was also obtained by modification with DDA for the reflux time of 48 h, whereas other reflux times led to intercalated structures. Morphological observations were in a good consistency with the results of productivity and molecular weight measurement. Degree of fragmentation for the M2 was higher than that for D48 nanocomposite due to its higher yield and molecular weight. The dynamic mechanical behavior and thermal degradation of D24 nanocomposite were distinct from those of D48 and D72 samples. It was originated from poor dispersion of the nanoclay in the matrix. On the contrary, M2-M6 samples showed similar behavior due to their similar in the morphology of ncnoclay. Furthermore, degree of crystallinity of the nanocomposites containing nanoclay modified by NH_3/MAO was higher than those of the samples treated with NH_3/DDA due to their lower content and exfoliated structures. The highest complex viscosity and storage modulus at low frequencies were observed for M6 because of good dispersion and relatively high amount of nanoclay in this nanocomposite. According to obtained results, it is concluded that modification conditions and chemical nature of the modifiers can considerably influence the polymerization, and activity of the catalyst system, structure and morphology of the prepared nanocomposite and as a result, properties of the product.

ACKNOWLEDGEMENTS

The authors gratefully acknowledge support of this work by the Iran National Science Foundation through Grant 92008258.

REFERENCES

1. Panupakorn P, Chaichana E, Praserthdam P, Jongsomjit B (2013) Polyethylene/clay nanocomposites produced by in situ polymerization with zirconocene/MAO catalyst. J Nanomater 2013: 1–9
2. Nikkhah SJ, Ramazani SA A, Baniasadi H, Tavakolzadeh F (2009) Investigation of properties of polyethylene/clay nanocomposites prepared by new in situ Ziegler–Natta catalyst. Mater Des 30: 2309–2315
3. Peacock A (2000) Handbook of polyethylene: structures: Properties, and applications. CRC Press
4. Taguet A, Cassagnau P, Lopez-Cuesta JM (2014) Structuration, selective dispersion and compatibilizing effect of (nano) fillers in polymer blends. Prog Polym Sci 39: 1526–1563
5. Das R, Banerjee SL, Kundu PP (2016) Fabrication and characterization of in situ graphene oxide reinforced high-performance shape memory polymeric nanocomposites from vegetable oil. RSC Adv 6: 27648–27658
6. Yazdaninia A, Khonakdar HA, Jafari SH, Asadi V (2016) Influence of trifluoropropyl-POSS nanoparticles on the microstructure, rheological, thermal and thermomechanical properties of PLA. RSC Adv 6: 37149–37159
7. Chen T, Yang H, Li W (2015) Phase structure and mechanical properties of disentangled ultra-high molecular weight polyethylene/polyhedral oligomeric silsesquioxane nanocomposites in a solid state. J Polym Res 22: 1–8
8. Zanjanijam AR, Bahrami M, Hajian M (2016) Poly (vinyl chloride)/single wall carbon nano-

tubes composites: Investigation of mechanical and thermal characteristics. J Vinyl Addit Technol 22: 128-133

9. Cai D, Song M (2015) Ultra-high enhancement in the toughness of polyethylene by exfoliated natural clay nanosheets. J Appl Polym Sci 132: 41314
10. Sánchez-Valdes S, Ramírez-Vargas E, Ramos de Valle LF, Martinez-Colunga JG, Romero-Garcia J, Ledezma-Perez AS, Mendez-Nonell J, Castañeda-Flores ME, Morales-Cepeda A (2016) Physical and mechanical properties of linear low density polyethylene/cycloolefin copolymer/layered silicate nanocomposite. Polym Compos 37: 3167-3174
11. Trifkovic M, Hedegaard AT, Sheikhzadeh M, Huang S, Macosko CW(2015) Stabilization of PE/PEO Cocontinuous Blends by Interfacial Nanoclays. Macromolecules 48:4631-4644
12. Raji M, Essabir H, Essassi EM, El Mokhtar Essassi, Rodrigue D, Bouhfid R, Qaiss AK (2016) Morphological, thermal, mechanical, and rheological properties of high density polyethylene reinforced with Illite clay. Polym Compos: 10.1002/PC.24096
13. Zare Y (2015) Estimation of material and interfacial/interphase properties in clay/polymer nanocomposites by yield strength data. Appl Clay Sci 115:61-66
14. Singh VP, Kapur GS, Choudhary V (2016) High-density polyethylene/needle-like sepiolite clay nanocomposites: Effect of functionalized polymers on the dispersion of nanofiller, melt extensional and mechanical properties. RSC Adv 6:59762-59774
15. Hakim S, Safajou-Jahankhanemlou M, Zeynali ME (2013) Polyethylene nanocomposite prepared by a metallocene catalyst supported on MMT using a new pretreatment method. J Polym Res 20:1-10
16. Ramazani SA A, Tavakolzadeh F (2008) Preparation of polyethylene/layered silicate nanocomposites using in situ polymerization approach. Macromol Symp 274: 65-71
17. Maneshi A, Soares JBP, Simon LC (2006) A Single-gallery model for the in situ production of polyethylene/clay nanocomposites. Macromol Symp 243: 277-286
18. Kaminsky W (2014) Metallocene based polyolefin nanocomposites. Materials 7:1995–2013
19. Maneshi A, Soares JBP, Simon LC (2011) An efficient in situ polymerization method for the production of polyethylene/clay nanocomposites: Effect of polymerization conditions on particle morphology. Macromol Chem Phys 212:2017–2028
20. Zapata PA, Belver C, Quijada R, Aranda P, Ruiz-Hitzky E (2013) Silica/clay organo-heterostructures to promote polyethylene–clay nanocomposites by in situ polymerization. Appl Catal A-Gen 453:142-150
21. Herrero M, Núñez K, Gallego R, CarlosMerino J,Pastor JM (2016) Control of molecular weight and polydispersity in polyethylene/needle-like shaped clay nanocomposites obtained by in situ polymerization with metallocene catalysts. Eur Polym J 75:125-141
22. Carrero A, van Grieken R, Suarez I, Paredes B (2012) Development of a new synthetic method based on in situ strategies for polyethylene/clay composites. J Appl Polym Sci 126:987-997
23. Xalter R, Pelascini F, Mülhaupt R (2008) Ethylene polymerization, on-line particle growth monitoring, and in situ nanocomposite formation using catalysts supported on arylsulfonic acid-modified boehmites. Macromolecules 41:3136-3143
24. Abedi S, Abdouss M, Daftari-Besheli M, Min KE, Seo KH, Noh SK(2013) Highly exfoliated PE/Na^+ MMT nanocomposite produced via in situ polymerization by a catalyst supported on a novel modified Na^+ MMT. Polym Bull 70:2783-2792
25. Abedi S, Abdouss M, Nekoomanesh-Haghighi M, Sharifi-Sanjani N (2013) New clay-supported Ziegler–Natta catalyst for preparation of PE/Clay nanocomposites via in situ polymerization. J Appl Polym Sci 128:1879-1884
26. Maneshi A, Soares JBP, Simon LC (2011) Polyethylene/clay nanocomposites made with metallocenes supported on different organoclays. Macromol Chem Phys 212:216-228

27. Scott SL, Peoples BC, Yung C, Rojas RS, Khanna V, Sano H, Suzukie T, Shimizu F (2008) Highly dispersed clay–polyolefin nanocomposites free of compatibilizers, via the in situ polymerization of α-olefins by clay-supported catalysts. Chem Commun 4186-4188
28. Zapata P, Quijada R, Covarrubias C, Moncada E, Retuert J (2009) Catalytic activity during the preparation of PE/clay nanocomposites by in situ polymerization with metallocene catalysts. J Appl Polym Sci 113:2368-2377
29. Lee D, Kim H, Yoon K, Min KE, Seo KH, Noh SK (2005) Polyethylene/MMT nanocomposites prepared by in situ polymerization using supported catalyst systems. Sci Technol Adv Mater 6:457-462
30. Huang Y, Yang K, Dong J (2006) Copolymerization of ethylene and 10-undecen-1-ol using a montmorillonite-intercalated metallocene catalyst: synthesis of polyethylene/montmorillonite nanocomposites with enhanced structural stability. Macromol Rapid Commun 27:1278-1283
31. Ren C, Du X, Ma L, Wang Y, Tang T (2010) The role of polymerizable organophilic clay during preparing polyethylene nanocomposite via filling polymerization. J Appl Polym Sci 117:1646-1657
32. Liu C, Tang T, Huang B (2004) Zirconocene catalyst well spaced inside modified montmorillonite for ethylene polymerization: Role of pretreatment and modification of montmorillonite in tailoring polymer properties. J Catal 221:162-169
33. Ren C, Du X, Ma L, Wang Y, Zheng J, Tang T (2010) Preparation of multifunctional supported metallocene catalyst using organic multifunctional modifier for synthesizing polyethylene/clay nanocomposites via in situ intercalative polymerization. Polymer 51: 3416-3424
34. Leone G, Bertini F, Canetti M, Boggioni L, Stagnaro P, Tritto I (2008) In situ polymerization of ethylene using metallocene catalysts: Effect of clay pretreatment on the properties of highly filled polyethylene nanocomposites. J Polym Sci Pol Chem 46:5390-5403
35. Ray S, Galgali G, Lele A, Sivaram S (2005) In-situ polymerization of ethylene with bis (imino) pyridine iron (II) catalysts supported on clay: the synthesis and characterization of polyethylene–clay nanocomposites. J Polym Sci Pol Chem 43:304-318
36. Huang Y, Yang K, Dong J-Y (2007) An in situ matrix functionalization approach to structure stability enhancement in polyethylene/montmorillonite nanocomposites prepared by intercalative polymerization. Polymer 48: 4005-4014
37. Liu C, Tang T, Zhao Z, Huang B (2002) Preparation of functionalized montmorillonites and their application in supported zirconocene catalysts for ethylene polymerization. J Polym Sci Pol Chem 40:1892-1898
38. Jeong DW, Hong DS, Cho HY, Woo SI (2003) The effect of water and acidity of the clay for ethylene polymerization over Cp_2ZrCl_2 supported on TMA-modified clay materials. J Mol Catal A-Chem 206:205-211
39. Novokshonova LA, Kovaleva NY, Ushakova TM, Meshkova IN, Krasheninnikov VJ, LadyginaI TA, Leipunskii O, Zhigach AN, Kuskov ML (2005) Partially hydrolyzed alkylaluminums as the active heterogenized components of metallocene catalysts. Kinet Catal 46:853-860
40. Weiss K, Wirth-Pfeifer C, Hofmann M, Botzenhardt S, Lang H, Brüning K, Meichel E (2002) Polymerisation of ethylene or propylene with heterogeneous metallocene catalysts on clay minerals. J Mol Catal A-Chem 182:143-149
41. Suga Y, Maruyama Y, Isobe E, Suzuki T, Shimizu F (1994) Catalyst for polymerizing an olefin and method for producing an olefin polymer. US 5308811 A
42. Alikhani A, Hakim S, Nekoomanesh M (2017) Modified preparation of HDPE/clay nanocomposite by in situ polymerization using a metallocene catalyst. Iran Polym J 26: 721-731
43. Huang Y, Qin Y, Dong J, Zhao X, Hu X(2012) PE/OMMT nanocomposites prepared by in situ polymerization approach: Effects of OMMT-intercalated catalysts and silicate modifications. J Appl Polym Sci 123:3106–3116
44. Maneshi A (2010) In-situ ethylene polymerization with organoclay-supported metallocenes for

the preparation of polyethylene-clay nanocomposites. PhD Thesis, University of Waterloo, Ontario, Canada

45. Kiliaris P, Papaspyrides CD (2010) Polymer/layered silicate (clay) nanocomposites: an overview of flame retardancy. Prog Polym Sci 35:902-958
46. Jamshidi S (2014) Mechanical, rheological and thermal properties of polyethylene (PE)/clay nanocomposite for rotomolded containers. Master Thesis, University of Calgary, Canada
47. Zhao C, Qin H, Gong F, Feng M, Zhang S, Yang M (2005) Mechanical, thermal and flammability properties of polyethylene/clay nanocomposites. Polym Degrad Stab 87:183-189
48. Jahani Y, Valavi A, Ziaee F (2015) Reactive melt modification of polyethylene by ethyl acrylate/acrylic acid copolymers: Rheology, morphology and thermal behavior. Iran Polym J 24:449-458
49. Ma J, Zhang S, Qi Z, et al (2002) Crystallization behaviors of polypropylene/montmorillonite nanocomposites. J Appl Polym Sci 83:1978-1985
50. Xie Y, Yu D, Kong J, Fan X, Qiao W (2006) Study on morphology, crystallization behaviors of highly filled maleated polyethylene-layered silicate nanocomposites. J Appl Polym Sci 100:4004-4011
51. Lee J-H, Jung D, Hong C-E, et al (2005) Properties of polyethylene-layered silicate nanocomposites prepared by melt intercalation with a PP-g-MA compatibilizer. Compos Sci Technol 65:1996-2002
52. Hyun YH, Lim ST, Choi HJ, Jhon MS (2001) Rheology of poly (ethylene oxide)/organoclay nanocomposites. Macromolecules 34:8084-8093